Adaptive Tactile Force Control in a Parallel Gripper With Low Positioning Resolution

Nicola A. Piga, *Member, IEEE*, and Lorenzo Natale, *Senior Member, IEEE*

***Abstract*—In this letter we develop an adaptive tactile force controller for a parallel gripper with low positioning resolution. We show both mathematically and experimentally that a standard integral controller is not suited to control the force in a closed-loop fashion as it induces oscillations in the system. Therefore, we devise an adaptive controller that exploits the tactile readings to model the relationship between the gripper position and the tactile force readings and uses it to avoid the oscillations. We provide a mathematical characterization of the proposed controller and extensive experimental results with objects from the YCB model set. The results show that the proposed controller outperforms the integral controller and reduces the oscillations in a substantial way. Moreover, the position/force relationships are estimated with good precision. We also test the proposed controller as part of a cascaded architecture for the control of the sliding velocity of an object. The experiment shows the effectiveness of the controller for tasks where it is required to track a reference force profile from a high-level controller.**

***Index Terms*—Adaptive control, force control, force and tactile sensing, object properties estimation.**

I. Introduction

PARALLEL grippers are ubiquitous tools in robotics where they are used to enable robot manipulators to grasp objects [1], [2], [3] and perform in-hand object manipulation tasks [4], [5], [6] such as controlling the sliding motion of an object [7].

The characteristics of a gripper, excluding fingers length and maximum force ratings, are usually considered non-critical for the successful execution of grasping actions. Indeed, as long as the gripper can close its fingers around the object and hold the configuration steadily, the grasping action will succeed - under the assumption that the grasp pose and the grasp strength have been planned accurately so as not to violate friction constraints at the contact points.

However, when a gripper is equipped with tactile sensors for force sensing and control, other characteristics of the gripper become crucial. One of such specifications is the positioning resolution, depending on the smallest variation in the fingers position that the gripper system allows the user to command. The higher the resolution is, the better the ability of the inner control system of the gripper to track the position inputs provided by the user. In turn, the quality of the position tracking affects the effectiveness of any force regulation control system that the user implements on top of the position controller.

In this letter we investigate the behavior of tactile force control feedback strategies in a parallel jaw gripper when the positioning resolution cannot be neglected. Our contributions are as follows:

- a positioning resolution-aware modelling of the gripper/object system and a mathematical characterization of the shortcomings of closing the force control loop using a plain integral controller;
- an adaptive control strategy, and its mathematical characterization, which, based on an online prediction of the tactile measurements, mitigates the above shortcomings;
- an extensive experimental evaluation of the tactile force tracking and prediction errors of the proposed architecture for 18 objects, including objects from the standard YCB model set [8];
- the integration of the controller within a cascaded control system for a higher-level task, namely the control of the sliding velocity of an object.

II. Related Work

To the best of our knowledge, the problem that we consider has not been extensively explored in the past literature, with few exceptions.

In [9], the authors consider a voltage-controlled gripper in contact with an object, where the contact force cannot be modulated if the input voltage is too small. This dead zone-like behavior makes the contact force jump above and below the desired reference when the control loop is closed with the measured force.

In the technical report [10], the authors identify another source of oscillations within a tactile force control architecture in the slow response exhibited by certain types of tactile sensors. When a large force is applied and then removed, the sensor may still detect its presence for a very short time, leading to oscillations.

A gripper-like system, made of two gripping pads mounted on the arms of a humanoid robot, is considered in [11]. The gripping force regulation is subject to unwanted oscillations in presence of small errors between the desired and measured tactile force.

Manuscript received 4 April 2023; accepted 8 July 2023. Date of publication 19 July 2023; date of current version 25 July 2023. This letter was recommended for publication by Associate Editor Paolo Di Lillo and Editor Clement Gosselin upon evaluation of the reviewers' comments. *(Corresponding author: Nicola A. Piga.)*

The authors are with the Istituto Italiano di Tecnologia, Humanoid Sensing and Perception, 16163 Genoa, Italy (e-mail: nicola.piga@iit.it; lorenzo.natale@iit.it).

This letter has supplementary downloadable material available at https://doi.org/10.1109/LRA.2023.3297061, provided by the authors.

Digital Object Identifier 10.1109/LRA.2023.3297061

This work is licensed under a Creative Commons Attribution 4.0 License. For more information, see https://creativecommons.org/licenses/by/4.0/

In the above works, the commonly adopted solution to mitigate oscillations is to compare the desired tactile force with the *measured* one and revoke the control action when they are close enough, e.g. in [9] is proposed to wait until the 98% of the desired value is reached. Nonetheless, in [9] they tested the proposed approach only qualitatively and with two kind of compliant surfaces, in [10] no experimental results are provided while [11] do not focus extensively on the problem of oscillations. Moreover, in [9] it is not clear how to adapt the solution taking into account the width of the dead zone.

In this work, we propose a more structured approach to the problem of oscillations due to the low positioning resolution of a parallel gripper. Specifically, we design an adaptive controller which decides when to disable the control action by comparing the desired tactile force with a *future prediction* that is estimated online without prior knowledge of the object. Our approach can be easily adapted to grippers with different characteristics once the positioning resolution is known. Furthermore, we provide qualitative and quantitative results of experiments on several objects with diverse mechanical properties.

III. Integral and Adaptive Force Control

In this section we provide a mathematical characterization of the gripper/object system, and demonstrate that a conventional integral controller generates oscillations. Next, we propose an adaptive controller which avoids the oscillations. To simplify the analysis, we assume a linear, known, relationship between the position of the gripper and the tactile reading when the fingers are in contact with the object. In the next Section, we show that these assumptions can be removed using an online estimation procedure.

A. System Description

We assume that the system of interest consists of a 1-DOF parallel gripper, whose fingers are in contact with an object $\mathcal{O}$. The fingers of the gripper are equipped with tactile sensors providing a reading proportional to the force normal to the surface of the sensor.

Let $p_k \in \mathbb{R}$ be the gripper aperture at time k, $f_k^l \in \mathbb{R}$ and $f_k^r \in \mathbb{R}$ the tactile readings of the left and right fingers, respectively, expressed in raw sensor units. In the following, we consider the mean tactile force $f_k = (f_k^l + f_k^r)/2$ exerted by the gripper.

The inner control system of the gripper exposes a control input u_k which changes the gripper aperture p_k. Ideally, we would describe the input-output relationship of a parallel gripper as plain linear, i.e. $p_k \approx u_k$. In this work, we instead consider the case where the input is discretized due to the positioning resolution:

$$p_k = \left\lfloor \frac{u_k}{\delta_p} \right\rfloor \delta_p = N_k \delta_p, \tag{1}$$

where $N_k \in \mathbb{N}$ and δ_p is the minimum displacement that can be commanded, i.e. the positioning resolution. We remark that the gripper aperture p_k varies in a continuous fashion while transitioning from one set-point to the next. In this respect, the purpose of (1) is to clarify that the system input u_k is subjected to discretization.

Given the above, the aim of this work is to design a control strategy u_k such that the tactile force f_k can track a desired profile f_k^d, while considering the constraint in (1).

B. Integral Control and Its Shortcomings

One possibility is to design a control law such that the *velocity* of the gripper is *proportional* to the error e_k

$$e_k = f_k^d - f_k \tag{2}$$

between the measured tactile force f_k and the desired one f_k^d. As several grippers only provide a position control mode, we integrate such velocity resulting in the following *integral* law

$$u_{k+1} = u_k + k_i e_k \Delta_t \tag{3}$$

for the *position* of the gripper, where Δ_t is the sampling time of the controller and $k_i > 0$.

In the following we assume a linear relationship between the measured tactile reading f and the gripper position p when the fingers are in contact with the object:

$$f(p) = c_0 + c_1 p. \tag{4}$$

Given (1)–(4), the error dynamics can be written as:

$$\begin{aligned} e_{k+1} &= -c_1 N_k(u_k, e_k)\delta_p + \left(f_{k+1}^d - c_0\right), \\ N_k(u_k, e_k) &= \left\lfloor \frac{u_k + k_i e_k \Delta_t}{\delta_p} \right\rfloor \in \mathbb{N}, \end{aligned} \tag{5}$$

where we assume $c_0 \geq 0$ and $c_1 > 0$.

The equilibrium points of the error dynamics can be studied by setting $e_{k+1} = e_k = e_{eq}$ and considering a steady reference f_{eq}^d. We indicate with $N_{k_{eq}}$ the value of N_k at the time k_{eq} when we assume the system is at equilibrium. The equilibrium points are as follows:

$$e_{eq} = -c_1 N_{k_{eq}} \delta_p + \left(f_{eq}^d - c_0\right). \tag{6}$$

Setting the error equal to 0 and recalling that $N_k \in \mathbb{N}$, it can be seen that the error vanishes if and only if

$$\left| \frac{f_{eq}^d - c_0}{c_1 \delta_p} \right| \in \mathbb{N}. \tag{7}$$

This condition depends on the desired target f_{eq}^d, the parameters c_0, c_1 and δ_p, that are out of the user control. Otherwise, the equilibrium error is different from zero. In the latter case, it can be shown that the equilibrium has an oscillatory behavior.

To show that, we first notice that $u^* = \frac{f_{eq}^d - c_0}{c_1}$ is the value of the control input that would make the error zero, in the ideal case $p_k = u_k$. Taking into account the constraint in (1), the position of the gripper that best approximates u^* is $\left\lfloor \frac{u^*}{\delta_p} \right\rfloor \delta_p$. Assuming, without loss of generality, that the gripper already moved *at least* by that amount, the corresponding equilibrium error is

$$e_{eq} = -c_1 \left\lfloor \frac{u_{k_{eq}}}{\delta_p} \right\rfloor \delta_p + \left(f_{eq}^d - c_0\right), \tag{8}$$

$$u_{k_{eq}} \in \left[\left\lfloor \frac{u^*}{\delta_p} \right\rfloor \delta_p, \left(\left\lfloor \frac{u^*}{\delta_p} \right\rfloor + 1 \right) \delta_p \right). \tag{9}$$

The actual value of e_{eq}, for any possible choice of $u_{k_{eq}}$ in (9), is:

$$e^+ = -c_1 \left\lfloor \frac{f^d_{eq} - c_0}{c_1 \delta_p} \right\rfloor \delta_p + \left(f^d_{eq} - c_0\right). \tag{10}$$

Using the fact that $\lfloor x \rfloor \leq x \ \forall x \in \mathbb{R}$ and $\lfloor x + n \rfloor = \lfloor x \rfloor + n \, \forall x \in \mathbb{R}, \forall n \in \mathbb{N}$, it is possible to prove that $e^+ > 0$.

Given that the error is positive, the control input in (3) will increase and eventually reach the set

$$\left[\left(\left\lfloor \frac{u^*}{\delta_p} \right\rfloor + 1\right)\delta_p, \left(\left\lfloor \frac{u^*}{\delta_p} \right\rfloor + 2\right)\delta_p\right), \tag{11}$$

for which the resulting error is:

$$e^- = -c_1 \left\lfloor \frac{f^d_{eq} - c_0}{c_1 \delta_p} \right\rfloor \delta_p + \left(f^d_{eq} - c_0 - c_1\delta_p\right). \tag{12}$$

Using the properties that $\lfloor x \rfloor = \lceil x \rceil - 1$ and $\lceil x \rceil \geq x \, \forall x \in \mathbb{R}$, it can be shown that $e^- < 0$. As a consequence, the control input will decrease and eventually go back inside the interval in (9), for which the error is again positive.

In summary, the error oscillates between the two values e^+ and e^-. This represents a non-ideal behavior for both the gripper and the object that is manipulated.

C. Adaptive Controller

In this section, we describe the proposed control strategy that aims at removing the oscillatory behavior.

The main idea is to evaluate a one step ahead *prediction* of the error, in the following e^m_{k+1}, that the system would achieve if the gripper had moved from the current configuration, *before* actually sending the command. If such prediction is lower than the current error, the control action is executed, as per (3), otherwise it is revoked. The control law is as follows:

$$u_{k+1} = u_k + \Delta_u,$$
$$\Delta_u = \begin{cases} k_i e_k \Delta_t & |e^m_{k+1}| < |e_k| \\ 0 & \text{otherwise.} \end{cases} \tag{13}$$

We define the prediction of the error as

$$e^m_{k+1} = f^d_{k+1} - f^m_{k+1}, \tag{14}$$

i.e., the difference between the desired tactile force f^d_{k+1} and a prediction of the force at step $k+1$, f^m_{k+1}. The latter is evaluated using the model in (4), assuming that the gripper had moved by an amount $\delta(e_k)$:

$$f^m_{k+1} = f\left(p_k + \delta(e_k)\right). \tag{15}$$

At first glance, a suitable choice for $\delta(e_k)$ seems to be the control action itself, $k_i e_k \Delta_t$. However, this choice is not sound for at least two reasons: i) the error prediction would depend on the gain k_i, which is undesirable ii) the error prediction would assume that the gripper command can assume any value, which is not true due to the constraint in (1). Instead, we propose to shape $\delta(e_k)$ such that it accounts for the number of steps required to reduce the force error given the resolution δ_p and the coefficient c_1 which converts a change in position to a change in force. Taking into account the sign of the error, we get:

$$\delta(e_k) = \text{sgn}(e_k) \left\lceil \frac{|e_k|}{c_1 \delta_p} \right\rceil \delta_p. \tag{16}$$

The use of the ceiling operator makes sure that the prediction always considers at least one step of the gripper, also in the case $|e_k|/c_1 < \delta_p$ when the error is already small compared to the positioning resolution. This is fundamental to understand the behavior of the error around the current position p_k and take the correct decision in (13).

Substituting (1) and (4), e^m_{k+1} evaluates to

$$\begin{aligned} e^m_{k+1} &= f^d_{k+1} - f^m_{k+1} \\ &= f^d_{k+1} - (c_0 + c_1 p_k + c_1 \delta(e_k)) \\ &= -c_1 \text{sgn}(e_k) \left\lceil \frac{|e_k|}{c_1 \delta_p} \right\rceil \delta_p - c_1 \left\lfloor \frac{u_k}{\delta_p} \right\rfloor \delta_p + \left(f^d_{k+1} - c_0\right) \\ &= -\left(\text{sgn}(e_k) \left\lceil \frac{|e_k|}{c_1 \delta_p} \right\rceil + \left\lfloor \frac{u_k}{\delta_p} \right\rfloor\right) c_1 \delta_p + \left(f^d_{k+1} - c_0\right). \end{aligned} \tag{17}$$

We now analyze the behavior of the system at equilibrium. We remark that the definition of the equilibrium error in (8) is still valid as it does not depend on the specific definition of the control law, rather on the value $u_{k_{eq}}$. We also notice that

$$|e^+| + |e^-| = c_1 \delta_p, \tag{18}$$

a fact that will be useful in the following discussion.

We assume, without loss of generality, that the error configuration at equilibrium is $e_{eq} = e^+ > 0$. Two cases need to be discussed.

Case 1 $|e^+| < |e^-|$. By substituting $e_{eq} = e^+$, $f^d_{k+1} = f^d_{eq}$ in (17), and recalling that $u_{k_{eq}}$ satisfies (9), the prediction of the error is as follows:

$$e^m_{k_{eq}+1} = e^+ - \left\lceil \frac{e^+}{c_1 \delta_p} \right\rceil c_1 \delta_p. \tag{19}$$

Using the assumption that $|e^+| < |e^-|$ and combining it with (18), it can be found that

$$e^+ = |e^+| < \frac{c_1 \delta_p}{2}. \tag{20}$$

Substituting the above in (19) shows that

$$e^m_{k_{eq}+1} = e^+ - c_1 \delta_p, \tag{21}$$

hence

$$|e^m_{k_{eq}+1}| > \frac{c_1 \delta_p}{2}. \tag{22}$$

As a consequence $|e^m_{k_{eq}+1}| > |e^+|$ and, according to (13), $\Delta_u = 0$ and $u_{k_{eq}+1} = u_{k_{eq}}$. That is, the oscillation is avoided. Considering that $|e^+| < |e^-|$, this also represents the smallest error the system could reach given the constraint in (1).

Case 2 $|e^+| > |e^-|$. Using (18), the prediction of the error in (19) can be rearranged as follows:

$$e^m_{k_{eq}+1} = e^- + \left(1 - \left\lceil \frac{e^+}{c_1 \delta_p} \right\rceil\right) c_1 \delta_p. \tag{23}$$

Using the assumption that $|e^+| > |e^-|$ together with (18) it can be found that

$$|e^-| < \frac{c_1 \delta_p}{2} \tag{24}$$

and

$$\frac{c_1 \delta_p}{2} < |e^+| < c_1 \delta_p. \tag{25}$$

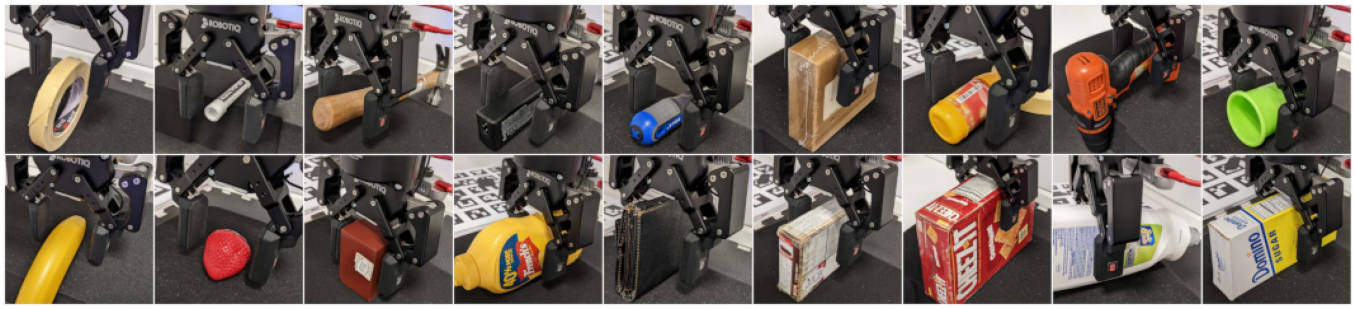

Fig. 1. The objects used for the tactile force tracking and prediction experiments. The relative configuration between the gripper fingers and the object is the one used to perform the experiments before the actual contact takes place.

Eq. (25) implies that

$$\left\lceil \frac{e^+}{c_1 \delta_p} \right\rceil = 1, \tag{26}$$

hence $e^m_{k_{eq}+1} = e^-$. As a consequence, $|e^m_{k_{eq}+1}| < |e^+|$ and, as per (13), $\Delta_u = k_i e^+ \Delta_t > 0$ and $u_{k_{eq}+1} > u_{k_{eq}}$.

As long as $u_{k_{eq}+i}$, $i > 0$, remains within the set in (9), the value of $e^m_{k_{eq}+i+1}$ is equal to $e^m_{k_{eq}+1}$, hence $|e^m_{k_{eq}+i+1}| < |e_{k_{eq}+i}| = |e^+|$ and the controller in (13) behaves as in (3). As already explained in Section III-B, in this condition the control input increases until the error eventually transitions from e^+ to e^-. Using a similar reasoning as in the Case 1, but taking into account that $|e^-| < |e^+|$ and that $u_{k_{eq}+i}$ now satisfies (11) instead of (9), it can be shown that $|e^m_{k_{eq}+1}| > |e^-|$. That is no more oscillations will occur and the error will be the smallest possible for the system given the constraint in (1).

IV. Tactile Measurement Prediction

A. Actual Implementation of the Measurement Prediction

The developments from the previous section assume that the parameters c_0 and c_1 in (4) are available and exact. In case the parameters are estimated, the latter assumption might not hold resulting in an incorrect prediction f^m_{k+1}. In this respect, we propose to substitute the term $c_0 + c_1 p_k = f(p_k)$ with the actual feedback from the sensor f_k resulting in

$$f^m_{k+1} = f_k + c_1 \delta(e_k). \tag{27}$$

As a consequence, the prediction does not depend on c_0 anymore and it benefits from the knowledge of the actual reading from the sensor at time k.

Furthermore, the relationship $f(p)$ in (4) assumes linearity with respect to the gripper position p. A more general solution, that corresponds to (27) in the linear case, is

$$f^m_{k+1} = f_k + \frac{\partial f(p)}{\partial p}\bigg|_{p=p_k} \delta(e_k), \tag{28}$$

where f can be nonlinear and a first-order approximation of the function f is used (under the assumption that $\delta(e_k)$ is small enough to make the higher-order terms of the function negligible).

B. Polynomial Estimation of the position/force Relationship

In order to evaluate the prediction f^m_{k+1} it is required to know the position/force relationship $f(p)$ in (4). In general, such a function depends both on the nature of the material of the gripper fingers and that of the object to be manipulated.

In this work we propose to estimate the function f online while the controller in (13) is running but asynchronously. Specifically, we monitor the value of the gripper position p_k and every time it assumes a value that is different from the previous one, we collect a sample

$$z = (p_k, f_k) \tag{29}$$

and add it to the set of measurements Z. For each new sample z in the set, we estimate f using least-squares under the assumption that it has a polynomial form:

$$f(p) = \sum_{i=0}^{N} c_i p^i. \tag{30}$$

The result of the estimation process are the coefficients c_i. In order to guarantee that the estimation can run online, we limit the number of samples $|Z|$ to a given maximum and discard old samples.

Given the structure of the estimate, the first-order approximation in (28) can be easily evaluated in closed form as

$$f^m_{k+1} = f_k + \left(\sum_{i=1}^{N} i c_i p_k^{i-1} \right) \delta(e_k). \tag{31}$$

In order to make the estimate independent of the actual size of the object, it is also possible to substitute p_k with the relative displacement with respect to the position p_c at which the first contact with the object occurred:

$$\tilde{p}_k = p_k - p_c \geq 0. \tag{32}$$

V. Experimental Results

In this section we present the results of several experiments aimed at assessing the effectiveness of the proposed controller.

We first discuss, qualitatively and quantitatively, the tracking performance of the controller when fed with a reference signal f^d_k. We repeat the experiment with several objects from the YCB Model Set [8] and other household objects. We show all the objects used in the experiments in Fig. 1. We compare with a

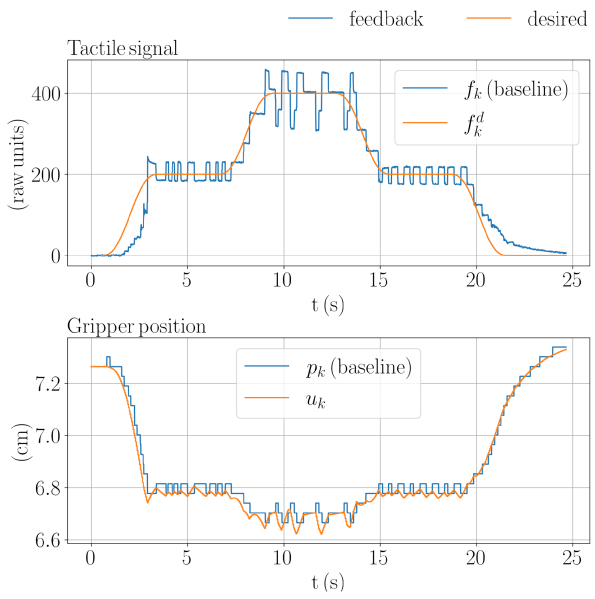

Fig. 2. Outcome of one of the tactile force tracking experiments when using the baseline controller for the object "Stacking block". Top: tactile signal. Bottom: position of the gripper (8.5 cm is the maximum width of the gripper).

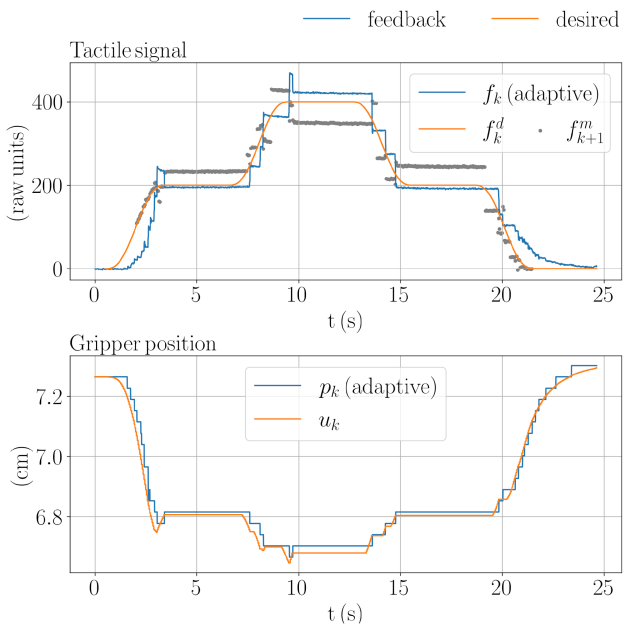

Fig. 3. Outcome of one of the tactile force tracking experiments when using the adaptive controller for the object "Stacking block". Top: tactile signal with predictions (gray dots). Bottom: position of the gripper.

baseline consisting in the same controller without the adaptation mechanism, i.e. the controller described in Section III-B.

Next, we assess the performance of the tactile measurement prediction process, described in Section IV, in order to analyze its role independently of the control part. We also provide qualitative results showing the shape of the estimated function f for several objects.

To conclude, we test the proposed controller on a high-level control task, consisting in the regulation of the velocity of an object while it slides between the fingers of the gripper. We compare also in this case with the baseline and discuss the advantages of the proposed solution.

A. Description of the Setup

All the experiments are carried out on a Franka Emika Panda robot equipped with a Robotiq 2F-85 parallel gripper. We emphasize that the positioning resolution of the gripper, $\delta_p = 0.37\,\text{mm}$, is of several order of magnitude higher than that of other, more precise, grippers. As such, it represents a suitable candidate for our experiments, as the constraint in (1) is particularly relevant for this gripper.

The gripper fingers are covered with magnetic-based uSkin 3D tactile sensors [12]. Each finger contains an array of 24 sensors organized in 4 rows and is covered by a soft silicone membrane. The scalar left and right tactile signals f_k^l and f_k^r are obtained by evaluating the average of all sensors along the z direction, i.e. the one perpendicular to the finger plane. We remark that the sensors are not calibrated and all the reported numbers are expressed using raw sensor units.

As regards the tuning of the controller in (3), we chose the gain k_i separately for each object, as for each sensor/object interface the closed loop system exhibits different stability properties. This fact can also be seen using the theory of LTI systems in the ideal case in which $p_k = u_k$ and the relationship $f(p)$ is linear. Specifically, we increased the gain as much as possible, in order to maximize the bandwidth, while avoiding instability. In order to have a fair comparison, we directly transferred the same gains to the adaptive controller in (13), so as to study the effect of the adaptation mechanism independently.

Considering the tactile measurement prediction, we set $N = 2$ in (30) and $|Z| = 100$, as the results showed that these were appropriate choices for all the objects.

The software that implements both controllers is made available with an open-source license.[1]

B. Results on Tactile Force Tracking

The aim of this experiment is to assess the ability of the controller to track a given force reference f_k^d. We modulate the reference signal in order to explore different force targets, namely 200 and 400 in sensor units. For each target, we keep the reference constant for several seconds in order to assess the presence of oscillations. We repeat the experiment ten times using 18 objects, reported in Table I.

In Fig. 2, we report the outcome of a single trial when using the baseline controller. When the reference is kept constant, the gripper position and the tactile signal oscillate as we anticipated in Section III-B.

In Fig. 3, we instead show the outcome of the adaptive controller alongside with the predictions f_{k+1}^m. At steady state, the oscillations are avoided thanks to the information provided by the predictions f_{k+1}^m.

In Table I, we provide quantitative results for all the objects. In the second column we report the error e between the desired

[1][Online]. Available: https://github.com/hsp-iit/adaptive-tactile-force-control

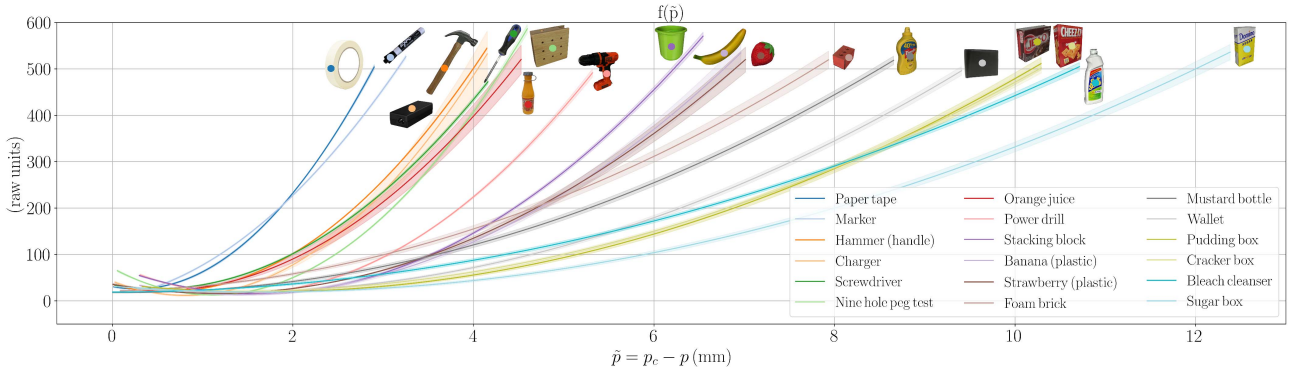

Fig. 4. Examples of possible position/force relationships $f(\tilde{p})$ estimated using the data collected during the tactile force tracking experiments. Each is represented with a mean curve, obtained from the data of ten experiments, together with 95% confidence intervals.

TABLE I
RESULTS OF THE TACTILE FORCE TRACKING EXPERIMENTS IN TERMS OF THE TRACKING ERROR AND ITS FIRST TIME DERIVATIVE. RESULTS ARE EXPRESSED AS MEAN (STD)

Metric	$e\downarrow$		$\dot{e}\ (1/s)\ \downarrow$		$\dot{e}_{const}\ (1/s)\ \downarrow$	
Method	Baseline	Adaptive	Baseline	Adaptive	Baseline	Adaptive
Paper tape*	36.9 (0.8)	**33.3** (1.9)	321.4 (11.6)	**166.1** (11.0)	329.6 (20.9)	**116.3** (20.6)
Marker	**34.0** (0.5)	35.1 (1.0)	232.4 (6.1)	**148.5** (1.9)	233.0 (12.8)	**101.6** (11.0)
Hammer	35.4 (0.7)	**33.8** (0.6)	267.1 (11.7)	**154.1** (4.6)	266.9 (16.4)	**81.3** (9.0)
Charger*	46.7 (5.9)	**38.2** (2.9)	393.4 (67.6)	**180.9** (47.7)	401.0 (70.9)	**80.9** (17.0)
Screwdriver	38.3 (0.9)	**33.2** (1.7)	285.6 (12.7)	**127.6** (4.8)	325.0 (10.9)	**72.1** (6.7)
Peg test	49.9 (2.7)	**40.2** (2.1)	414.6 (31.8)	**212.9** (26.9)	459.8 (36.8)	**128.9** (39.1)
Orange j.*	**26.4** (0.7)	27.1 (4.0)	214.7 (8.2)	**161.7** (56.8)	229.1 (7.6)	**116.9** (76.5)
Power drill	41.5 (1.0)	**38.5** (1.4)	286.1 (17.2)	**167.8** (11.9)	308.7 (21.8)	**131.2** (21.4)
Stacking b.	40.0 (4.4)	**32.6** (2.0)	338.3 (57.5)	**191.4** (37.7)	379.3 (84.6)	**122.2** (44.2)
Banana	29.3 (2.2)	**25.6** (2.0)	229.6 (33.1)	**159.3** (30.4)	241.2 (61.8)	**96.3** (16.4)
Strawberry	31.0 (1.2)	**30.1** (1.0)	185.8 (18.9)	**127.7** (14.4)	172.1 (30.9)	**83.9** (23.0)
Foam brick	**18.6** (0.4)	20.5 (0.5)	109.0 (4.1)	**89.6** (3.4)	107.7 (5.6)	**61.0** (7.8)
Mustard b.	21.6 (1.2)	**21.3** (0.9)	146.2 (11.6)	**129.0** (15.4)	124.3 (10.9)	**80.9** (11.7)
Wallet*	27.9 (0.7)	**23.9** (0.6)	177.2 (11.2)	**108.3** (12.8)	194.4 (16.1)	**86.8** (13.5)
Pudding box	22.2 (1.1)	**20.9** (0.3)	127.4 (18.0)	**100.1** (9.1)	117.3 (30.5)	**66.4** (9.1)
Cracker box	28.6 (0.2)	**27.9** (0.5)	96.2 (6.4)	**80.8** (4.8)	90.3 (8.3)	**61.3** (8.8)
Bleach c.	21.1 (0.4)	**20.5** (0.4)	114.3 (5.0)	**97.4** (6.6)	100.3 (7.6)	**82.9** (10.8)
Sugar box	21.1 (2.9)	**20.0** (1.7)	135.9 (38.1)	**103.2** (28.2)	144.3 (62.6)	**75.5** (36.9)
ALL	31.7 (9.0)	**29.0** (6.7)	226.4 (95.9)	**139.2** (36.8)	234.7 (110.0)	**91.5** (22.2)

*Object not from the YCB Model Set.

TABLE II
RESULTS OF THE TACTILE MEASUREMENT PREDICTION EXPERIMENTS IN TERMS OF THE PREDICTION ERROR. RESULTS ARE EXPRESSED AS MEAN (STD)

Object	$e_{pred}\downarrow$	Object	$e_{pred}\downarrow$
Paper tape*	26.7 (0.2)	Banana	16.5 (2.0)
Marker	21.1 (0.2)	Strawberry	19.2 (0.5)
Hammer	21.2 (0.2)	Foam brick	13.9 (0.1)
Charger*	33.9 (0.9)	Mustard bottle	12.6 (0.2)
Screwdriver	19.8 (0.2)	Wallet*	9.8 (0.2)
Peg test	34.5 (0.3)	Pudding box	8.1 (0.2)
Orange juice*	22.6 (0.1)	Cracker box	8.2 (0.1)
Power drill	23.0 (0.3)	Bleach cleanser	7.3 (0.1)
Stacking block	38.4 (0.4)	Sugar box	5.8 (0.1)
ALL	19.0 (9.5)		

*Object not from the YCB Model Set.

and achieved force averaged over the trajectory time instants and over all trials. With few exceptions, the proposed controller achieves a better performance.

Most of the advantage of using the adaptive mechanism is clear from the derivative of the error $\dot{e}$, that we estimated using all the data of each experiment. The derivative of the error reports, although not exclusively, on the steadiness of the control action during constant reference phases. The proposed controller always outperforms the baseline achieving, on average, a reduction of $\approx 39\%$. In the last column, we restrict our attention to the constant reference phases of the trajectory, indicated as $\dot{e}_{\text{const}}$. The average reduction is $\approx 61\%$.

In Fig. 4 we report a sample of the position/force polynomial relationships in (30) estimated during the execution of the force tracking experiments. Each relationship is reported as a function of the relative displacement $\tilde{p}$ introduced in (32). For each object, we show the mean of the estimates obtained from ten experiments and the 95% confidence intervals. As one might expect, solid objects appear in the leftward part of the plot, as the force builds up earlier when the gripper closes against them. Conversely, hollow and more deformable objects, or softer ones, like the foam brick, appear in the center/rightmost part as the gripper needs to close more, up to ≈ 1.2 cm, to exert a similar force on them.

C. Results on Tactile Measurement Prediction

In this section, we discuss the performance of the online tactile measurement predictor presented in Sections III-C, IV-A, and IV-B. To this end, we setup a specific experiment where the gripper is commanded to close by small amounts δ_p in open loop until the tactile signal f_k is approximately equal to 400, in sensor units. For each step, we compare the predicted force f^m_{k+1}, obtained by setting $\delta(e_k) = \delta_p$ in (28), with the actual tactile signal achieved *after* the gripper has completed the step motion. We repeated the experiment ten times for each object. An example of the outcome is shown in Fig. 5.

In Table II, we report the average prediction error e_{pred} averaged over all trials. When considering all the objects, the average error is in the order of 20 sensor units corresponding to the 5% of the dynamic range considered in the experiment.

D. Results on Closed-Loop Object Sliding

In this section, we present the results of an experiment where the proposed controller is used as part of a cascaded architecture in order to control the sliding velocity of an object. The architecture is shown in Fig. 6.

We assume that the object can only translate along one direction during the sliding motion due to the interaction between the gravity force and the friction force between the object and the fingers of the gripper. We also assume that the object cannot rotate. The object velocity v_k is estimated online with a Kalman Filter [13] using the position of a fiducial marker attached

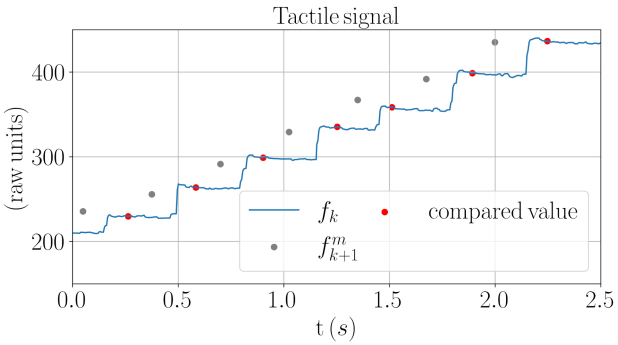

Fig. 5. Outcome of one of the tactile measurement prediction experiments. Each prediction, indicated with a grey dot, is compared to the tactile signal obtained when the gripper has actually moved by δ_p, indicated with a red dot on its right.

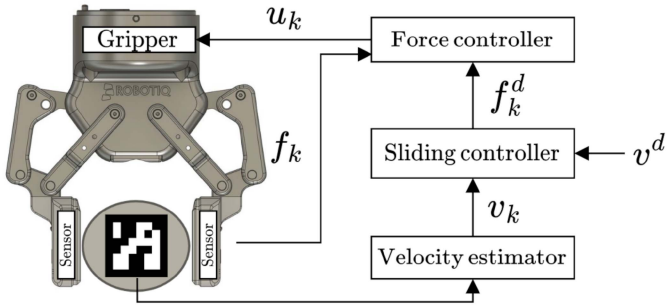

Fig. 6. A scheme representing the cascaded control architecture employed for the closed-loop object sliding experiments.

Fig. 7. The experimental setup during the execution of a sliding experiment with the "bottle" object.

to the object as the measurement. Furthermore, we make the hypothesis that the object needs to slide at a given constant velocity v^d.

Given the desired velocity v^d and the velocity feedback v_k, the sliding controller should provide a reference f^d_k to the force controller, such that the velocity error $e_{v,k} = v^d - v_k$ is minimized. Taking inspiration from the controller presented in [7], we design a two-stage PID controller to achieve the above goal. The first stage, termed *pre-sliding*, uses a PID controller to regulate the absolute force until the velocity v_k has reached a given pre-sliding velocity $v^{pre} < v^d$:

$$f^d_k = f^d_{k-1} + \text{PID}^{pre}\left(v^{pre} - v_k\right). \tag{33}$$

We indicate with f^* the value of the measured force f_k at the time the velocity reached the pre-sliding velocity.

The second stage uses a PID controller to regulate the force around the value f^* in order to reach the desired velocity v^d and compensate for external disturbances:

$$f^d_k = f^* + \text{PID}(e_{v,k}). \tag{34}$$

In order to perform the experiments we used a bottle of rigid plastic, shown in Fig. 7, filled up such that its weight was enough to make it slide between the fingers of the gripper. We performed ten experiments using both the baseline controller and the proposed adaptive controller to track the desired force f^d_k provided by the sliding controller. During the experiment, we also assess the ability of the controller to react to external disturbances by adding a weight on top of the bottle and removing it after a predefined time.

We set $v^{pre} = 0.05\,\text{cm/s}$ and $v^d = 0.1\,\text{cm/s}$. For the pre-sliding stage we set the gains of the PID controller as follows: $k^{pre}_p = 0$, $k^{pre}_i = 10^3$, $k^{pre}_d = 5 \times 10^3$. For the actual sliding, we set them to $k_p = 0.0$, $k_i = 2 \times 10^4$ and $k_d = 5 \times 10^3$.

We remark that at the beginning of the experiment the object does not move as the initial desired force f^d_0 is set to a value such that the object is firmly grasped by the gripper and it does not slide. In our experiments we set $f^d_0 = 300$.

In Fig. 8, in the top row, we compare the desired velocity with that achieved using both controllers. Each plot comprises the mean curve, averaged on all the experiments, and the 95% confidence intervals. The performance of both controllers is similar although, when using the adaptive controller, the error is sometimes slightly larger and more spread around the mean. When considering the corresponding behavior of the low-level force control, shown in Fig. 9 for one of the ten experiments, we can observe that the baseline controller induces persistent oscillations around the desired reference, while the oscillations are avoided with the adaptive controller.

In summary, the adaptive controller helps reduce the oscillations although at the cost of increasing the velocity error and its variance. This depends on the working principle of the adaptive controller, that is the possibility to disable the control loop, i.e. setting $\Delta_u = 0$ in (13), if the next control action is deemed not useful to reduce the force tracking error. While this mechanism removes the oscillation, at the same time it reduces the overall responsiveness of the system. Nonetheless, if the performance degradation is compatible with the constraints of the user and if the oscillations are to be avoided, the adaptive controller still represents a valuable alternative.

As additional experiments, we repeated our tests with a different target velocity $v^d = 0.25\,\text{cm/s}$. We kept all the other parameters unchanged. We report the results in the bottom row of Fig. 8. We also provide a video of the experiments, including tests on a different object, the hammer, which has different mechanical properties than the bottle.

E. Limitations and Future Directions

The performance of the proposed force controller depends significantly on the choice of the relationship $f(p)$. If the function is not estimated correctly, the force predictor f^m_{k+1} could underestimate or overestimate the actual force achieved by the system resulting in a wrong control decision. A possible future research direction could investigate how to detect if the estimated position/force relationship is wrong, imprecise or needs more samples to be refined, and how to recover from these situations.

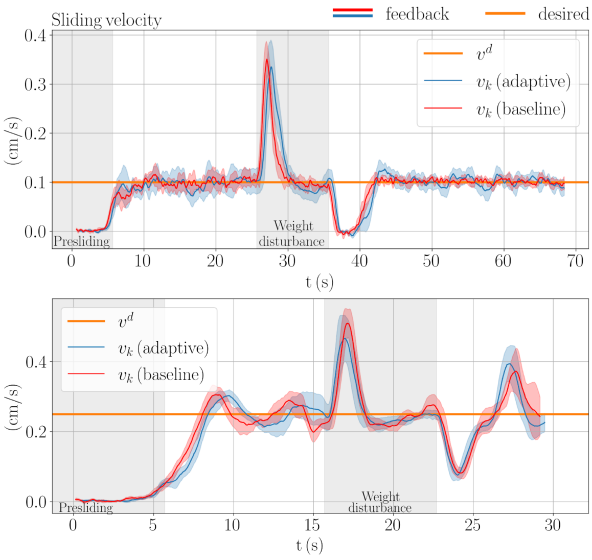

Fig. 8. Outcome of the sliding experiment with $v^{pre} = 0.05\,\mathrm{cm/s}$ and target velocities $v^d = 0.1\,\mathrm{cm/s}$ (top row) and $0.25\,\mathrm{cm/s}$ (bottom row). Each plot comprises a mean curve, averaged over ten experiments, and 95% confidence intervals.

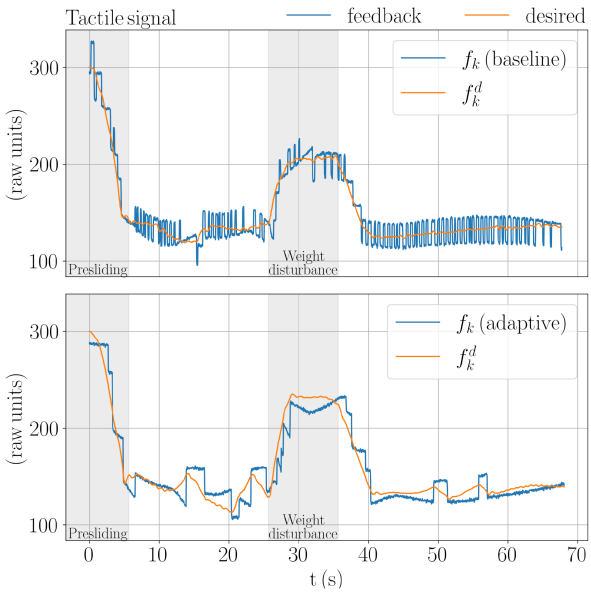

Fig. 9. Desired and achieved tactile force signal during the sliding experiment with $v^d = 0.1\,\mathrm{cm/s}$ when using the baseline (top row) and adaptive controller (bottom row).

Moreover, we plan to study how visual inputs combined within learning techniques could be used to provide a prior for the position/force relationship even before the interaction between the gripper and the object has occurred. This extension could be useful to reduce the number of tactile samples required to properly estimate the relationship. At the same time, the tactile readings might be used to refine the visual model so that it becomes more aligned with the objects the robot interacts with more often.

VI. Conclusion

In this letter we proposed an adaptive tactile force controller for grippers with low positioning resolution. We demonstrated, both mathematically and by means of experiments on a real gripper, that the proposed controller outperforms a plain integral tactile force controller by reducing the steady state oscillations, due to the low positioning resolution, and in terms of force tracking error and its derivative. The proposed controller can be used with different objects as proved by our experiments, carried out on a consistent number of objects from the standard YCB model set. Additional experiments on controlling the velocity of an object, that slides between the fingers of the gripper, showed that the proposed controller can be used as inner loop of a cascaded control architecture for higher-level control tasks.

Acknowledgment

The authors would like to thank Alessandro Altobelli, Fabrizio Bottarel, Gabriele M. Caddeo, Ugo Pattacini and Jonathan K. Woolfrey for the helpful discussions on the theory presented in this work.

References

[1] R. Newbury et al., "Deep learning approaches to grasp synthesis: A review," *IEEE Trans. Robot.*, 2023, early access, doi: 10.1109/TRO.2023.3280597.
[2] Z. Xie, X. Liang, and C. Roberto, "Learning-based robotic grasping: A review," *Front. Robot. AI*, vol. 10, 2023, Art. no. 1038658.
[3] M. Sundermeyer, A. Mousavian, R. Triebel, and D. Fox, "Contact-GraspNet: Efficient 6-DoF grasp generation in cluttered scenes," in *Proc. IEEE Int. Conf. Robot. Automat.*, 2021, pp. 13438–13444.
[4] Q. Li, O. Kroemer, Z. Su, F. F. Veiga, M. Kaboli, and H. J. Ritter, "A review of tactile information: Perception and action through touch," *IEEE Trans. Robot.*, vol. 36, no. 6, pp. 1619–1634, Dec. 2020.
[5] S. Cruciani, B. Sundaralingam, K. Hang, V. Kumar, T. Hermans, and D. Kragic, "Benchmarking in-hand manipulation," *IEEE Robot. Automat. Lett.*, vol. 5, no. 2, pp. 588–595, Apr. 2020.
[6] M. Costanzo, G. De Maria, and C. Natale, "Two-fingered in-hand object handling based on force/tactile feedback," *IEEE Trans. Robot.*, vol. 36, no. 1, pp. 157–173, Feb. 2020.
[7] Y. Chen, C. Prepscius, D. Lee, and D. D. Lee, "Tactile velocity estimation for controlled in-grasp sliding," *IEEE Robot. Automat. Lett.*, vol. 6, no. 2, pp. 1614–1621, Apr. 2021.
[8] B. Calli, A. Singh, A. Walsman, S. Srinivasa, P. Abbeel, and A. M. Dollar, "The YCB object and model set: Towards common benchmarks for manipulation research," in *Proc. Int. Conf. Adv. Robot.*, 2015, pp. 510–517.
[9] D. Castro, L. Marques, U. Nunes, and A. de Almeida, "Tactile force control feedback in a parallel jaw gripper," in *Proc. IEEE Int. Symp. Ind. Electron.*, 1997, vol. 3, pp. 884–888.
[10] C. A. Salter and J. S. Baras, "Real time control for NASA robotic gripper," Dept. of Elect. Eng. and Syst. Res. Center, Univ. of Maryland, College Park, MD, USA, Tech. Rep. NASA-CR-187957, Mar. 1990.
[11] Y. Han, B. Jiang, and G. S. Chirikjian, "Design, calibration, and control of compliant force-sensing gripping pads for humanoid robots," *J. Mechanisms Robot.*, vol. 15, no. 3, 2023, Art. no. 031010.
[12] T. P. Tomo et al., "A modular, distributed, soft, 3-axis sensor system for robot hands," in *Proc. IEEE-RAS 16th Int. Conf. Humanoid Robots*, 2016, pp. 454–460.
[13] R. E. Kalman, "A new approach to linear filtering and prediction problems," *Trans. ASME- J. Basic Eng.*, vol. 82, pp. 35–45, 1960.

Open Access funding provided by 'Istituto Italiano di Tecnologia' within the CRUI CARE Agreement